Electronic Supplementary Material (ESI) for Nanoscale.

Supporting Information

Crystalline Phosphorus Fibers: Controllable Synthesis and Visible-Light-Driven Photocatalytic Activity

Zhurui Shen[a,b], ZhuoFeng Hu[a], Wanjun Wang[a], Yecheng Li[a], Siu-Fung Lee[a], Donald K. L. Chan[a], Ting Gu[a], Jimmy C. Yu[a*]

a, Department of Chemistry, The Chinese University of Hong Kong, Shatin, New Territories, Hong Kong, China & Shenzhen Research Institute, The Chinese University of Hong Kong, Shenzhen, China
b, Key Laboratory for Advanced Ceramics and Machining Technology of Ministry of Education, Tianjin University & School of material Science and Engineering, Tianjin University, Tianjin 300072, PR China
** Corresponding author, E-mail: jimyu@cuhk.edu.hk*

Materials and Methods

Details about the tools and materials

a, Purification of red phosphorus: 2 g of commercial red phosphorus was added into 15 mL H_2O, and hydrothermally treated at 200 ^oC for 12 h in 25 mL autoclave to clear the oxide layers.

b, Silicon nanowires wafers: The silicon nanowires wafers used in this article were prepared based on the widely used "HF-etching" method [s1]. The commercial silicon wafers (Zhejiang Lijing Co. Ltd.) were cut into small pieces (20×8 mm) and cleaned by deionized (DI) water and acetone for times before etching. Then, the small silicon wafers were put into the reaction tube and etched in the HF-$AgNO_3$ solution (0.01 M HF, 0.001M $AgNO_3$) for 30 min. The as-prepared silicon nanowires wafers were cleaned using HNO_3 (5 M) solution, DI water successively and dried by N_2 flowing.

d, α-titanium (Ti) wafers: Ti wafers were prepared by cutting the commercial Ti sheets into small pieces (20×8 mm) and cleaned by dilute HNO_3, deionized (DI) water and acetone for times before using.

e, Technical details: The size of quartz capsule should be carefully kept, we have ever used the larger quartz capsule (4 times of volume) and some white phosphorus by-product was produced and autoignited to broke the nanostructures; when broking the quartz capsule, it was better to wrap the capsule by old newspaper to avoid the spattering of the quartz fragments.

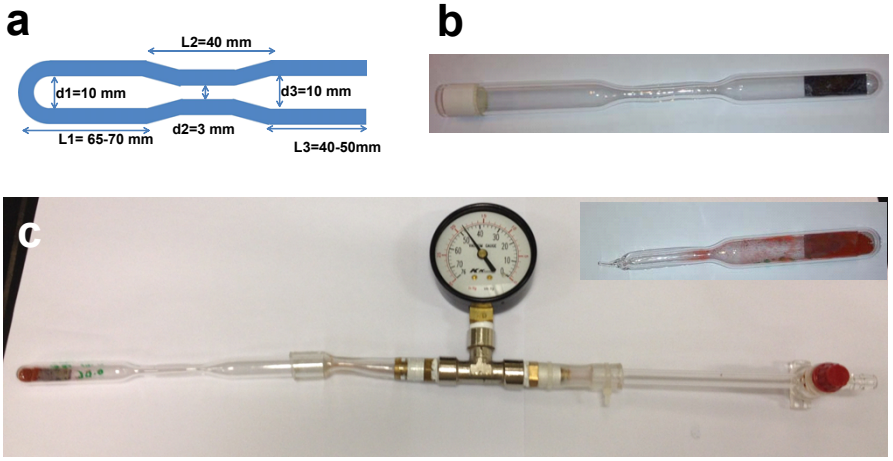

Figure S1. The quartz capsule and tools used in this study: a, The dimensions of the quartz capsule. b, a picture showing the placement of the substrate in the capsule before molding, c, the tools and capsule used for vacuum control, inset picture of (c) the sealed capsule after loading red phosphorus and evacuation.

S1. V. Sivakov, G. Andra, A. Gawlik, A. Berger, J. Plentz, F. Falk and S. H. Christiansen, *Nano Lett.***2009**, 9,1549-1554.

Synthesis. In a typical synthesis, 50-150 mg purified commercial red phosphorus was placed in a home-made quartz capsule (Figure S1, aid by Shenzhen Qihui. Co. Ltd.) with an appropriate substrate (e.g. p-Si(100) nanowires wafers). Then, under a low vacuum condition (-0.03 Mpa to -0.09 Mpa, high purity N_2 99.99 % filling before pumping), the capsule was sealed and heated in a furnace with the temperature of 550 ^oC, The elevating/ decreasing rates of temperature were set to 5^oC/min. The as-prepared products were obtained by broking the capsules, rinsing with dilute NaOH (0.5M) and DI water and finally drying in N_2 flow. The details see Section S1 and FigureS1. The yield of CVD synthesis: c.a. 1 wt% for one wafer, products grew on both sides of silicon wafers.

Characterization. SEM was measured on a FEI Quanta 400 microscope. The TEM, HRTEM and SAED were measured by a Philips Tecnai F20 instrument and a CM-120 microscope (Philips, 120 kV) coupled with a HAADF detector and an EDX spectrometer (Oxford Instrument). The TEM samples were prepared by infiltrating the as-prepared wafers in ethanol with sonication for 5 min and then transferring the dispersion onto the carbon film covered Cu grids. TEM images were processed by Digital Micrograph (Gatan, USA). The powder XRD patterns were recorded on a Rigaku SmartLab X-ray diffractometer using Cu Kα irradiation (λ = 1.5406Å). The accelerating voltage and applied current were 40 kV and 40 mA. UV–vis diffuse reflectance spectra were achieved using a UV–vis spectrophotometer (Cary 100 scan spectrophotometers, Varian). The high pressure liquid chromatograph (HPLC) was performed using Waters TM600-486 instrument, the column was Ace5 C18, and the mobile phase was 70/30 acetonitrile/acetic acid buffer (5mM).

Photoconductivity test, photocatalytic experiments and OH radicals test. Photoelectric properties measurements were carried out on an electrochemical workstation (CHI 660C, Shanghai Chen Hua Instrument Company, China). A conventional three-electrode system was used for photoelectric properties test: the work electrode was connected with the as-prepared wafers directly, a Ag/AgCl electrode as the reference electrode and a platinum wire electrode as the counter electrode. The electrolyte solution was 0.1 M $NaSO_4$ in water. The photocurrent response to on–off cycles was recorded under the illumination of a fiber optics equipped with a tungsten lamp (Cole-Parmer illuminator, 41720 series). The light intensity was about 200 mW/cm^2.

Photocatalytic evaluation of red phosphorus allotropes under visible light (VL)

irradiation was performed using a 300 W xenon lamp with a UV cutoff filter ($\lambda < 420$ nm) as light source. The VL intensity was measured by a light meter (LI-COR, USA) and the light intensity for the experiments was fixed at 193 mW/cm^2. In a typical test, two pieces of red phosphorus allotropes wafers (20×8 mm) was placed in 20 mL 10 ppm RhB solution. Before irradiation, this solution was magnetically stirred in dark for 60 min to ensure the establishment of an adsorption/desorption equilibrium between the photocatalyst and organic pollutants. At different time intervals, 1.5 mL of the sample was collected and test using UV-vis spectrometer. The concentration of RhB was measured according to the absorbance at 550 nm.

The recycling experiments of fibrous phosphorus submicron fibers were performed under the same conditions.

For photocatalytic degradation of 2, 3, 6-trichlorophenol, 20 ppm 2, 3, 6-trichlorophenol was used, and other conditions were kept unchanged compared with RhB degradation experiments. The sample was test using High pressure liquid chromatograph (HPLC), the mobile phase was 70/30 acetonitrile/acetic acid buffer (5mM), the measuring peak was at 288 nm, and the remaining time of 2, 3, 6-trichlorophenol was 3.25 min. The concentration of sample was calculated based on the area of the peak.

For control experiment of red phosphorus nanoparticle, 2 mg red phosphorus nanoparticles (c.a. 200~500 nm, made by mechanical milling from the commercial red phosphorus) and 2 mg fibrous phosphorus fibers powder (scraped from the wafer) were used as the photocatalysts. Other reaction conditions were kept the same with the photocatalytic experiments described above.

A stock terephthalic acid solution with final concentrations of 4×10^{-4} M terephthalic acid and 2×10^{-3} M NaOH was prepared. Two pieces of red phosphorus allotropes wafers (20×8 mm) was placed in 20 mL of the stock solution. The solution was irradiated by a 300 W halogen lamp (with a 420 nm filter). At every 1 hour, 1.5 mL of the suspensions were collected and centrifugated. The resulted supernatants were subjected to PL measurements. Fluorescence spectra of generated 2-hydroxyterephthalic acid were measured on a Hitachi F-4500 fluorescence spectrophotometer with an excitation wavelength of 320 nm.

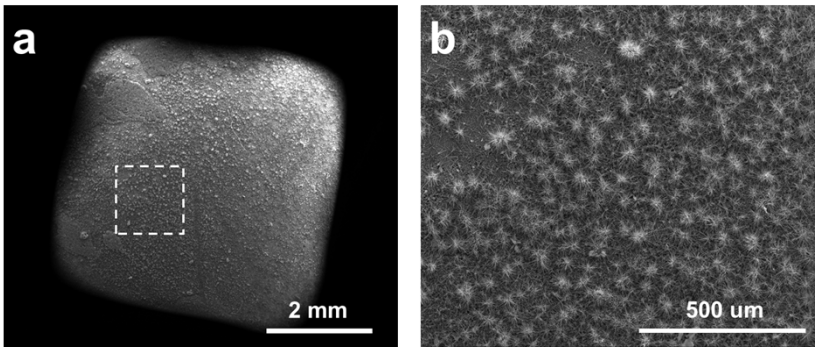

Figure S2. Low resolution SEM image of fibrous phosphorus submicron fibers obtained with 100mg red phosphorus , -0.06 Mpa and 550°C.

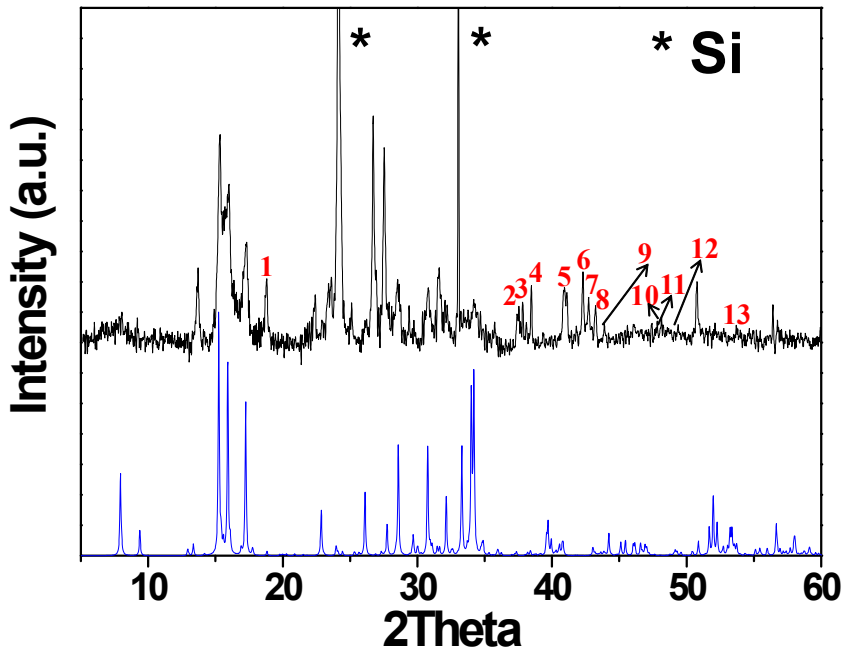

Figure S3. Enlarged picture of XRD pattern for fibrous phosphorus submicron fibers, blue curve was the simulated XRD pattern based on crystallographic data. The numbers denoted the weak peaks did not obviously correspond to the simulated one: 1-18.8° (*h k l*: -2 2 0); 2-37.3° (*h k l* : -4 3 1); 3-37.8° (*h k l* : 3 1 1); 4-38.2° (*h k l* : -4 4 0); 5-40.8° (*h k l* : 2 4 0); 6-42.3° (*h k l* : -2 2 0); 7-42.8° (*h k l* : 1 -6 1); 8-43.3° (*h k l* : 1 -4 3); 9-43.9° (*h k l* : -4 -4 2); 10-47.3° (*h k l* : 4 -2 2); 11-48.0° (*h k l* : -3 6 0); 12-49.5° (*h k l* : -5 3 2); 13-53.7° (*h k l* : 4 0 2).

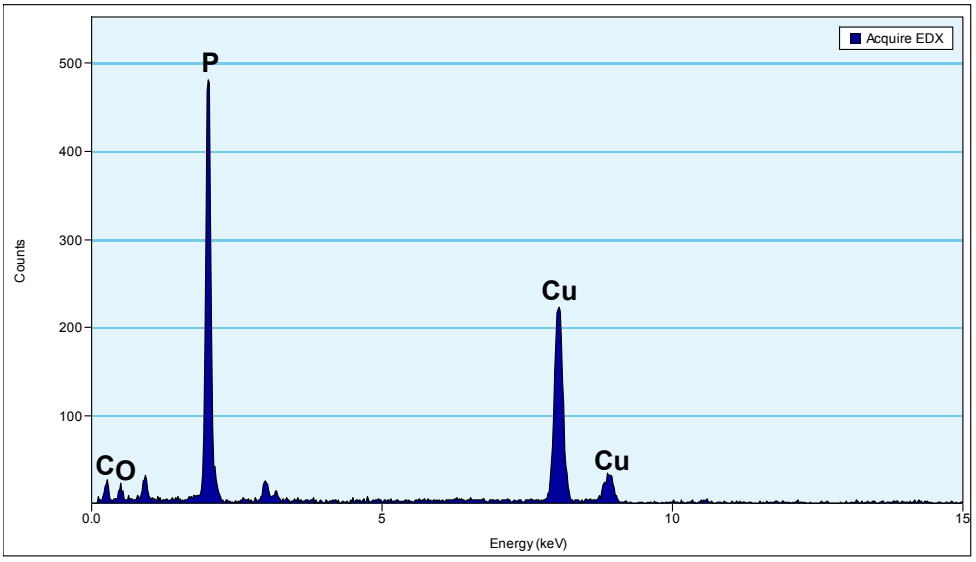

Figure S4. Representative EDX spectrum of fibrous phosphorus submicron fibers.

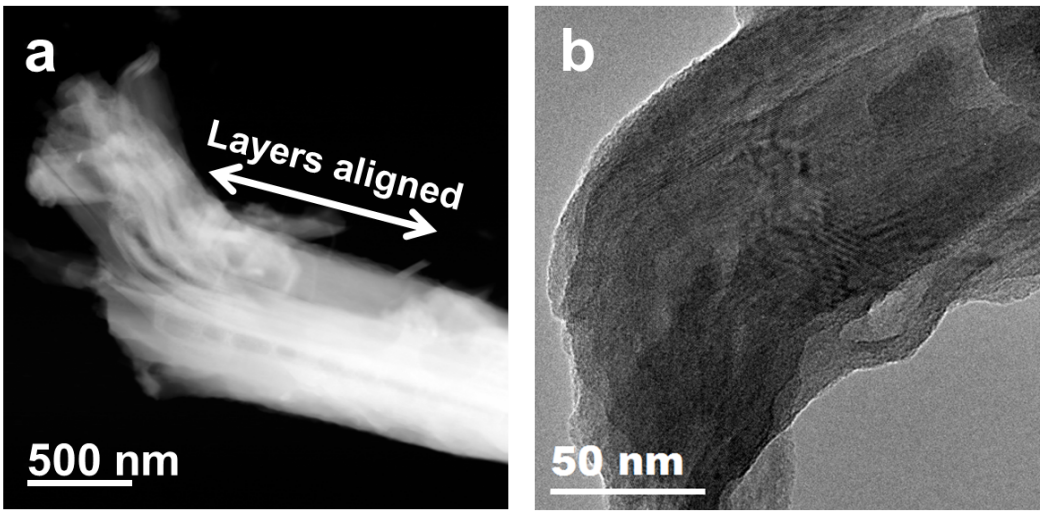

Figure S5. TEM analysis of layered structures in the fibrous phosphorus submicron fiber (a) HAADF-STEM image and (b) TEM image.

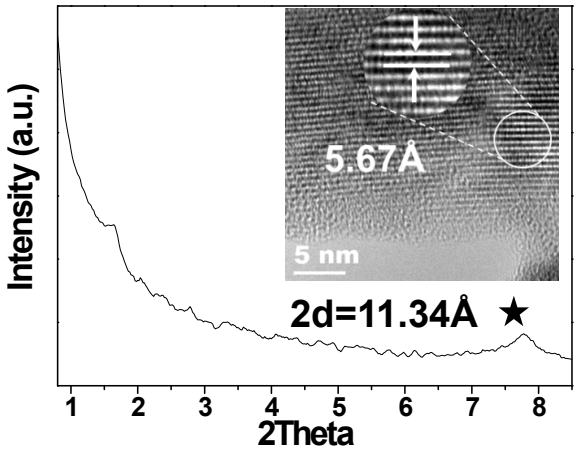

Figure S6. Small angle XRD pattern (0.6~8.5°) and the HRTEM image for the layered structure of fibrous phosphorus submicron fiber.

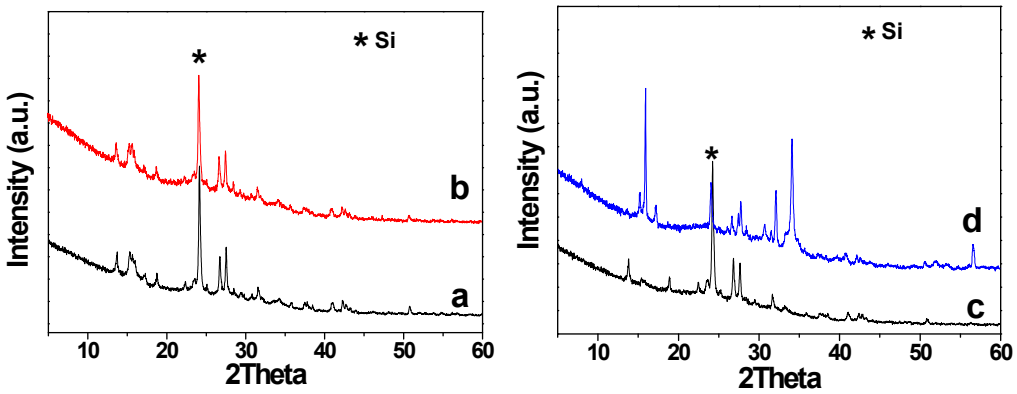

Figure S7. XRD patterns of fibrous phosphorus materials obtained with (a) 100 mg red phosphorus and vacuum of -0.03 Mpa, (b) 100 mg red phosphorus and vacuum of -0.09 Mpa, (c) 50 mg red phosphorus and vacuum of -0.06 Mpa, (d) 150 mg red phosphorus and vacuum of -0.06 Mpa.

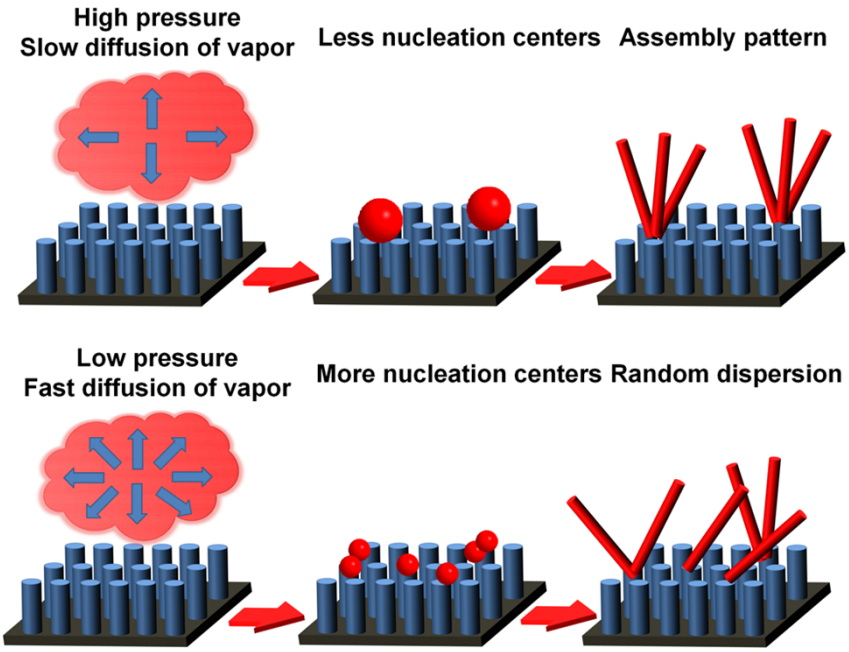

Scheme S1. Illustration for pressure control of fibrous phosphorus submicron fibers.

Scheme S1.

For CVD reaction, the vapor density of reaction species could greatly influence the nucleation and growth of product.[s2] Moreover, Kim *et al.* have found that at high pressure, the vapor would diffuse slowly to achieve a heterogeneous distribution.[s3] Therefore, a possible mechanism for pressure control was proposed:

"With the same amount of phosphorus in the systems, at high inner pressure (e.g. -0.03 Mpa, Scheme S1, up), the phosphorus vapor would diffuse slowly, and the vapor density is not homogenous. Therefore, less nucleation centers would be generated. Upon further cooling, crystal growth would dominate the reaction, and the assembly of fibers would grow from those nucleation centers. While at low inner pressure (e.g. -0.09 Mpa, Scheme S1, down), the phosphorus vapor would diffuse faster, and it will end up with a more homogeneous distribution. Therefore, more nucleation centers would be generated randomly, which would give rise to a random dispersion of fibers

S2. I. Avetissov, V.Kostikov,V.Meshkov, E.Sukhanova, M.Grishechkin, S.Belov and A.Sadovskiy, *J. Cryst. Growth*, 2014, **385**, 88.

S3. J. S. Kim, J. B.Yoo, D. H. Jang, D. H. Oh, Y. T. Lee, *J. Electro. Mater.* 1992, **21**, 251.

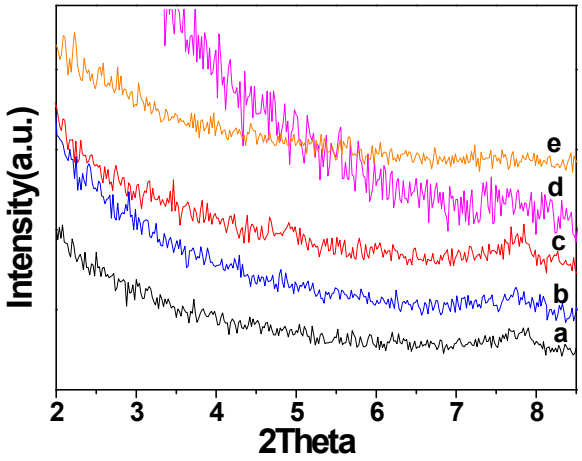

Figure S8. Small angle XRD patterns of red phosphorus allotropes obtained with (a) 100 mg red phosphorus and vacuum of -0.03Mpa, (b) 100 mg red phosphorus and vacuum of -0.09Mpa, (c) 150 mg red phosphorus and vacuum of -0.06Mpa, (d) 50 mg red phosphorus and vacuum of -0.06 Mpa. (e), red phosphorus nanorods obtained on α-Ti substrate with 100 mg red phosphorus and vacuum of -0.06 Mpa.

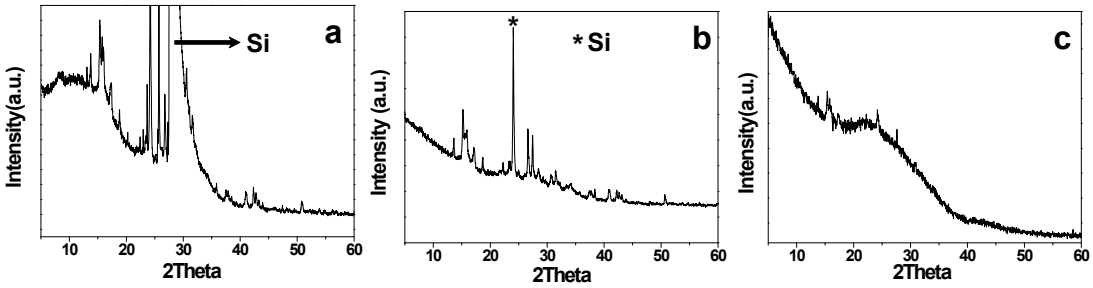

Figure S9. XRD patterns of red phosphorus alltropes obtained on (a) p-Si (111) nanowires wafer, (b) n-Si (100) nanowires wafer and (c) bare p-Si (100) wafer and at 550 ^{o}C, the quantity of red phosphorus is 100mg and the vacuum is -0.06 Mpa.

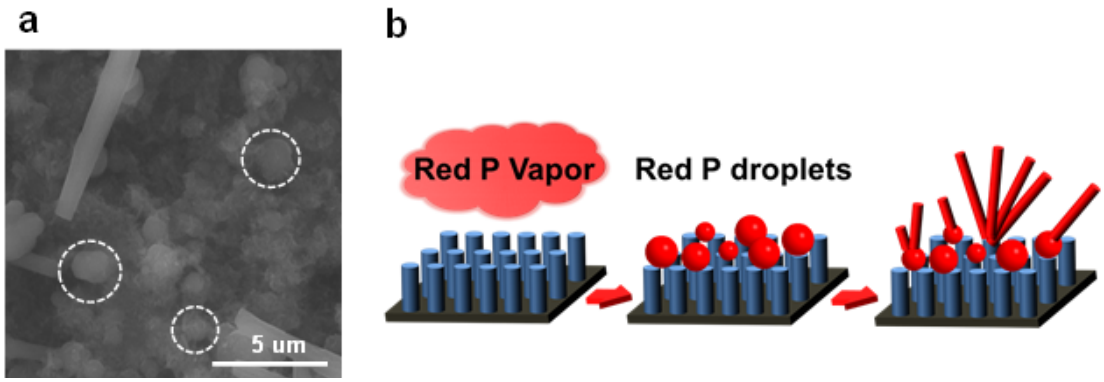

Scheme S2. (a) SEM image of red phosphorus particles; (b) diagram of dynamic growth process of fibrous phosphorus submicron fibers.

Scheme S2.

On the wafer, few spherical particles could be found among the fibrous phosphorus submicron fibers (Scheme S2a). This suggests that some phosphorus droplets might be condensed from its vapor with the decreasing of temperature. Then the droplets were adsorbed on the surface of the silicon wafer, and the phosphorus atoms would rearrange to achieve a lattice matching with silicon atoms. Finally, the most favorable fibrous phosphorus submicron fibers would grow from those gradually cooling phosphorus droplets. The whole process was illustrated in Scheme S2b, which is similar to some compounds grown by the CVD process.[s4, s5]

S4. W. D. Wang, Z. Zhang, Q. L. Liao, T. Yu, Y. W. Shen, P. F. Li, Y. H. Huang, Y. Zhang, *J. Cryst. Growth*, 2013, **363**, 247.

S5. S. Z. Zhou, Z. T. Lin, H. Y. Wang, T. Qiao, L. Y. Zhong, Y. H. Lin, W. L. Wang, W. J. Yang, G. Q. Li, *J. Alloys Compd.* 2014, **610**, 498.

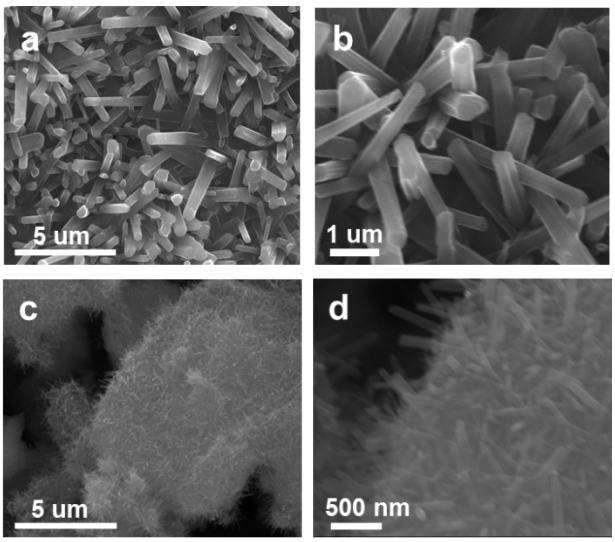

Figure S10. SEM images of (a, b) type II phosphorus submicron rods (100 mg red phosphorus, -0.06 Mpa , 550 ^{o}C , α-Ti wafer) and (c, d) Hittorf's phosphorus nanosheets (100 mg red phosphorus, -0.06 Mpa , 450 ^{o}C , p-Si (100) nanowires wafer).

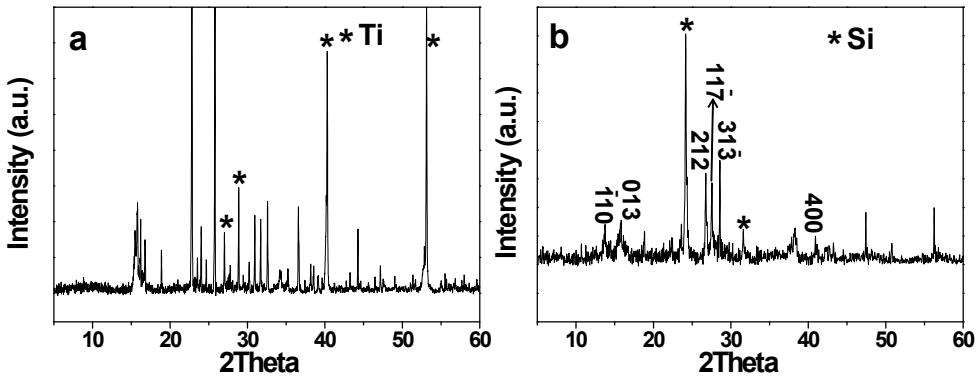

Figure S11. XRD patterns of (a) type II phosphorus submicron rods (100 mg red phosphorus, -0.06 Mpa , 550 ^{o}C , α-Ti wafer) and (b) Hittorf's phosphorus nanosheets (JCPDS: 44-0906, 100 mg red phosphorus, -0.06 Mpa , 450 ^{o}C , p-Si (100) nanowires wafer).

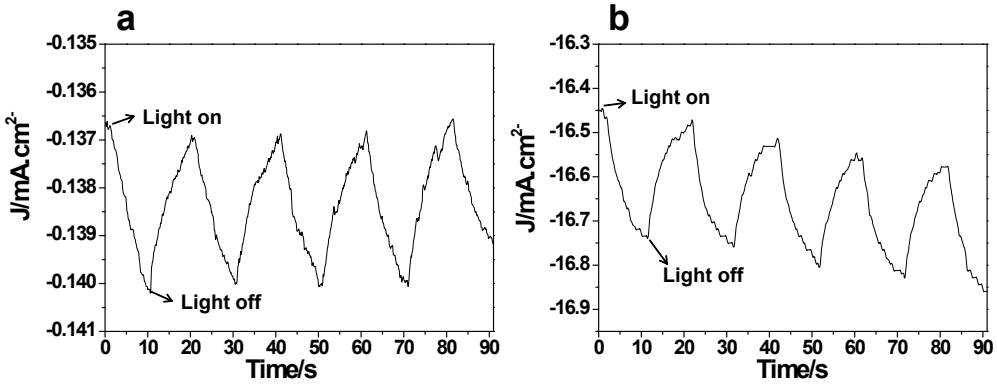

Figure S12. Photocurrent response of (a) fibrous phosphorus submicron fibers and (b) type II phosphorus submicron rods with the bias potential of -2 V (*vs.*Ag/AgCl).

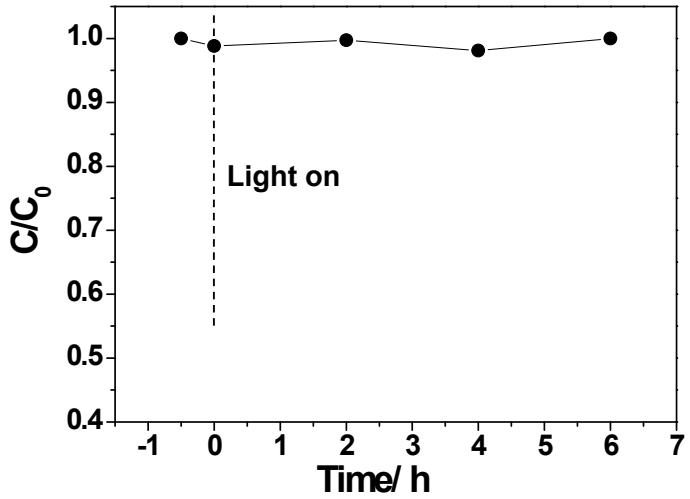

Figure S13 Typical photocatalytic performance of silicon nanowires wafer, via the degradation of RhB.

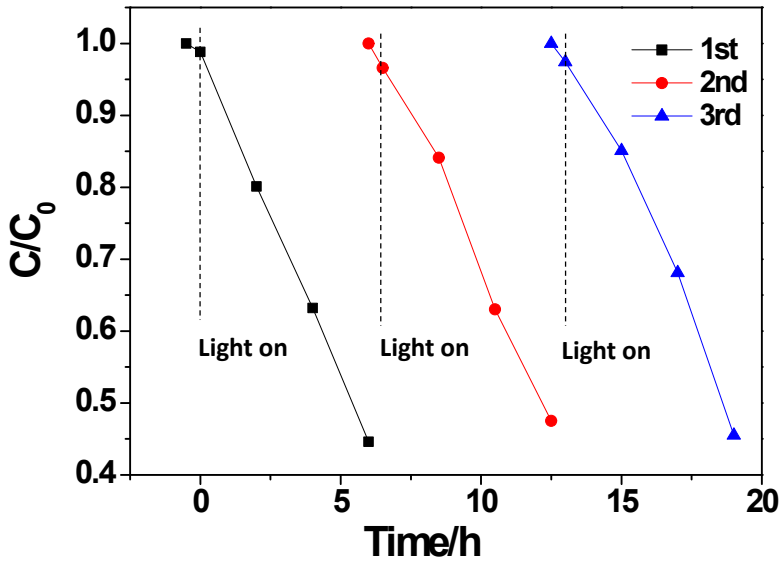

Figure S14 Recycled photocatalytic degradation of RhB over fibrous phosphorus submicron fibers (wafer).

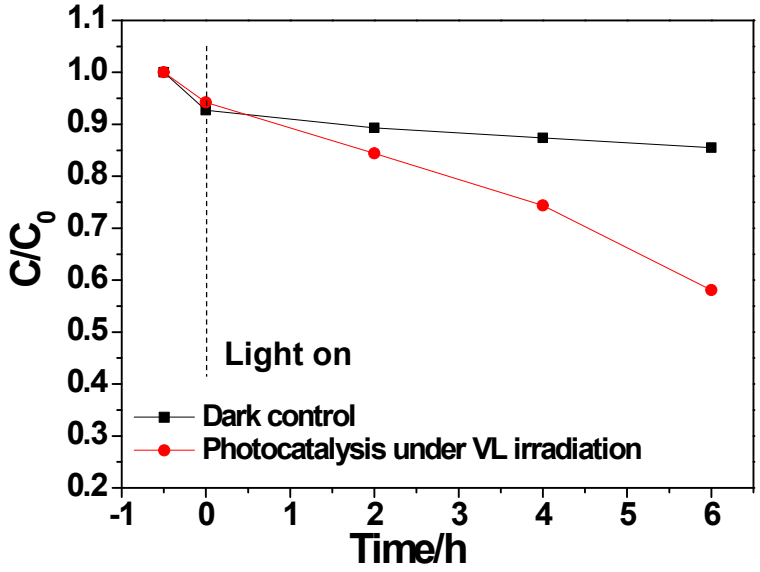

Figure S15 Photocatalytic performance of fibrous phosphorus submicron fibers (wafer), via the degradation of 2, 3, 6-trichlorophenol.

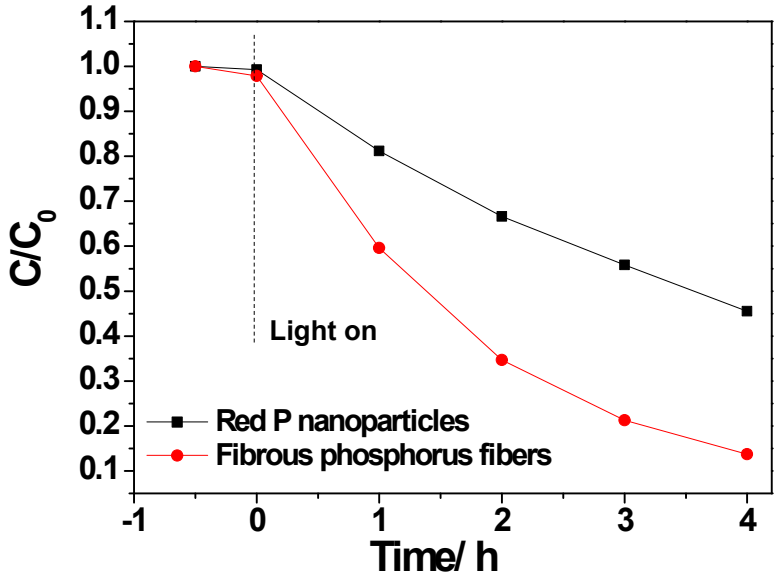

Figure S16. Photocatalytic performances of red phosphorus nanoparticles *vs.* fibrous phosphorus fibers powder via the degradation of RhB.